

Toward Multifunctional Materials Incorporating Stepladder Manganese(III) Inverse-[9-MC-3]-Metallacrowns and Anti-Inflammatory Drugs

Alketa Tarushi,[†] Antonios G. Hatzidimitriou,[†] Marta Estrader,[‡] Dimitris P. Kessissoglou,[†] Vassilis Tangoulis,^{*,§,✉} and George Psomas^{*,†,✉}

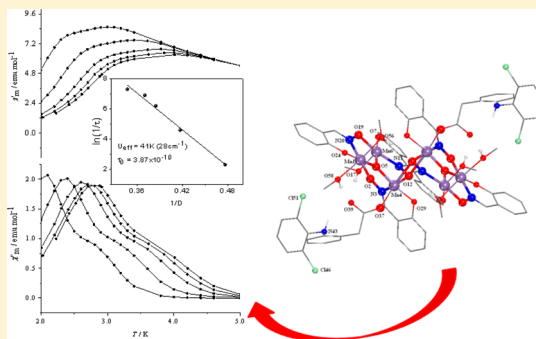
[†]Laboratory of Inorganic Chemistry, Faculty of Chemistry, Aristotle University of Thessaloniki, GR-54124 Thessaloniki, Greece

[‡]Departament de Química Inorgànica, Universitat de Barcelona, Diagonal 645, 08028 Barcelona, Spain

[§]Department of Chemistry, University of Patras, GR-26504 Patras, Greece

S Supporting Information

ABSTRACT: The interaction of $\text{Mn}(\text{ClO}_4)_2 \cdot 6\text{H}_2\text{O}$ with salicylaldoxime (H_2sao) in the presence of nonsteroidal anti-inflammatory drug (NSAID) sodium diclofenac (Nadcl) or indomethacin (Hindo) leads to the formation of the hexanuclear Mn(III) clusters $[\text{Mn}_6(\text{O})_2(\text{dicl})_2(\text{sao})_6(\text{CH}_3\text{OH})_6]$ (**1**) and $[\text{Mn}_6(\text{O})_2(\text{indo})_2(\text{sao})_6(\text{H}_2\text{O})_4]$ (**2**) both characterized as stepladder inverse-9-metallacrown-3 accommodating dicl^- or indo^- ligands, respectively. When the interaction of $\text{MnCl}_2 \cdot 4\text{H}_2\text{O}$ with Nadcl or Hindo is in the absence of H_2sao , the mononuclear Mn(II) complexes $[\text{Mn}(\text{dicl})_2(\text{CH}_3\text{OH})_4]$ (**3**) and $[\text{Mn}(\text{indo})_2(\text{CH}_3\text{OH})_4]$ (**4**) were isolated. The complexes were characterized by physicochemical and spectroscopic techniques, and the structure of complexes **1** and **2** was characterized by X-ray crystallography. Magnetic measurements (dc and ac) were carried out in order to investigate the nature of magnetic interactions between the magnetic ions and the overall magnetic behavior of the complexes.



1. INTRODUCTION

Polynuclear complexes of paramagnetic 3d- and 4f-metal ions have received tremendous attention over the last three decades or so, especially after the discovery that they can function as single-molecule magnets (SMMs), exhibiting the properties of bulk magnets but on the molecular level.^{1–9} After this discovery, the synthesis of multifunctional molecular materials has become one of the most appealing targets for synthetic chemists and material scientists. Traditional multifunctional systems, i.e., materials that combine multiple features, usually include various composite or nanocomposite materials in which one of the components plays the role of the matrix and the other components with various tailored properties are integrated into the matrix.^{8–11} The definition of multifunctional molecular materials relies on the combination of two or more physical properties in the same crystal lattice and covers a variety of different compounds.^{12–14} One of our goals of this interdisciplinary field of research is to synthesize and explore new classes of coordination compounds that may exhibit, besides single-molecule magnetism and ferromagnetism, important biological activity.

Metallacrowns (MCs) are a class of polynuclear complexes, which may be considered as molecular recognition agents and can be considered as the inorganic analogues of organic crown ethers. In brief, metallacrowns bear a cyclic structure analogous to crown ethers where the methylene carbons have been

replaced by transition-metal ions and nitrogen atoms;^{15,16} thus, the metallacrown ring is formed by repeating the $[-\text{O}-\text{N}-\text{M}-]$ pattern. In regard to the 9-MC-3 metallacrowns, two structural motifs have been reported, i.e., regular, when the oxygen atoms are oriented toward the center of the MC cavity leading to encapsulation of metal cations, and inverse, when the metal atoms are located toward the center of the MC cavity, thus hosting anions.^{15,16} Hydroxamic acids and oximes are usually used as constructing ligands of the metallacrown rings. For most of the reported inverse metallacrowns, the constructing ligands are multidentate oximes such as di-2-pyridyl-ketonoxime, phenyl-pyridyl-ketonoxime, and salicylaldoxime (H_2sao , Figure 1A) or its derivatives, which can act as bifunctional ligands by providing the nitrogen and the oxygen atoms for the formation of the metallacrown ring.

The doubly deprotonated ligand of salicylaldoxime (sao^{2-}) is potentially a tridentate binucleating ligand, which may be coordinated to the metal ions via its nitrogen and oxygen atoms participating in the formation of the metallacrown ring. In the literature, there are plenty of polynuclear trivalent metal complexes with salicylaldoxime as ligands, where the metal ion is Fe(III)^{17,18} or, in most cases, Mn(III).^{19–29} Concerning the nuclearity of these complexes, the majority of the existing

Received: March 12, 2017

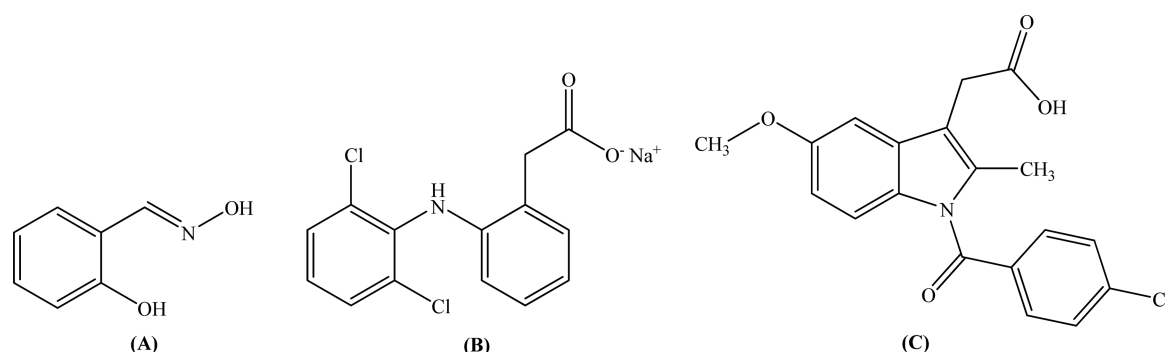


Figure 1. Syntax formula of (A) salicylaldoxime (H_2sao), (B) sodium diclofenac (Nadicl), and (C) indomethacin (Hindo).

72 reports include dinuclear,¹⁷ trinuclear,^{20,25} tetranuclear,^{18,23} and
73 hexanuclear^{22–29} complexes hosting diverse ligands such as
74 amides,²⁶ azides,^{27,28} halides,²⁹ perchlorate,²⁰ and diverse
75 carboxylate ligands.^{22–24}

76 Nonsteroidal anti-inflammatory drugs (NSAIDs) are among
77 the most frequently used analgesic, anti-inflammatory, and anti-
78 pyretic agents despite their known gastrointestinal and renal
79 side effects.³⁰ According to the characteristic chemical groups,
80 the chemical classes of NSAIDs include phenylalkanoate,
81 anthranilate, and salicylate derivatives bearing a carboxylic
82 group as well as oxicams, sulfonamides, and furanones.³¹ The
83 main biological target of the NSAIDs is the cyclooxygenase-
84 mediated production of prostaglandins,³² whereas NSAIDs
85 have shown synergism with respect to the activity of certain
86 antitumor drugs³³ and have presented antitumor activity
87 leading to cell death in cancer cell lines via apoptosis³⁴ or
88 other mechanisms.^{35,36} The study of the interaction with the
89 DNA (which is also a biological target of the anticancer drugs)
90 of NSAIDs and their compounds is of great importance as an
91 initial approach of their potential anti-inflammatory and anti-
92 cancer activity.^{37–39} Sodium diclofenac (Nadicl) and indome-
93 thacin (Hindo, Figure 1) are potent NSAIDs that belong to the
94 phenylalkanoic acid derivatives exhibiting favorable anti-
95 inflammatory, analgesic, and antipyretic properties,^{40–42} despite
96 gastrointestinal side effects such as ulceration and hemor-
97 rhage,⁴³ which limit the dose of NSAIDs. Sodium diclofenac is
98 mainly used in painful and inflammation conditions such as
99 rheumatoid arthritis, spondylitis, and osteoarthritis.⁴⁰ The
100 crystal structures of copper(II),^{44–47} manganese(II),^{48,49}
101 cadmium(II),⁵⁰ tin(IV),⁵¹ and nickel(II)⁵² complexes with
102 diclofenac ligands have been reported in the literature.
103 Indomethacin and its copper(II) complex are widely adminis-
104 tered in the clinical treatment of acute inflammation⁴¹ and
105 other medical conditions in humans.⁵³ A series of Cu(II)^{54–57}
106 and two tin complexes with indomethacin as a ligand⁵⁸ have
107 been reported in the literature.

108 Manganese is among the most important biometals because
109 of its presence in the active center of many enzymes of diverse
110 functionality.^{59,60} The manganese-containing compounds
111 SC-52608 and Teslascan are used in medicine as anticancer
112 and MRI contrast agents, respectively.⁶¹ In the context of bio-
113 inorganic chemistry, manganese compounds have been exam-
114 ined for their anticancer,^{62–64} antimicrobial,^{65–68} antifungal,⁶⁹
115 and antioxidant^{49,70} potencies, and in many cases, the results
116 were promising. Considering the metal-NSAID complexes,
117 there are reports on manganese complexes with the NSAIDs
118 diclofenac,^{48,49} mefenamic acid,⁷¹ niflumic acid,⁷² and tolfen-
119 namic acid.⁷⁰

Keeping in mind the biological significance of manga- 120
nese^{59–61} and the tentative biological activity of the NSAIDs 121
and their complexes,^{38,39,73} we present herein the synthesis and 122
the characterization of the manganese complexes with the 123
NSAIDs diclofenac and indomethacin in the presence or absence 124
of H_2sao . The presence of H_2sao led to the formation of the 125
hexanuclear complexes $[Mn_6(O)_2(dicl)_2(sao)_6(CH_3OH)_6]$ (1) 126
and $[Mn_6(O)_2(indo)_2(sao)_6(H_2O)_4]$ (2), which may be con- 127
sidered as inverse-[9-MC-3]₂metallacrowns and were charac- 128
terized by X-ray crystallography. The interaction of $MnCl_2 \cdot$ 129
 $4H_2O$ with the NSAIDs resulted in the mononuclear complexes 130
 $[Mn(dicl)_2(CH_3OH)_4]$ (3) and $[Mn(indo)_2(CH_3OH)_4]$ (4). All 131
complexes were characterized by physicochemical (elemental 132
analysis and molecular conductivity) and spectroscopic (IR 133
and UV-vis) techniques. The overall magnetic behavior of 134
compound 1 is ferromagnetic (FM), whereas at low temper- 135
atures the zero-field effect is important. According to the fitting 136
results of the susceptibility data, the ground state of the system 137
is $S = 4$ with many low-lying excited states. Furthermore, alter- 138
nating current (ac) magnetization measurements (both in-phase 139
and out-of-phase) show strong frequency-dependent behavior, 140
which is expected for an SMM. On the contrary, the overall 141
magnetic behavior of compound 2 is antiferromagnetic (AFM) 142
with no ac signals indicating a non-SMM character. 143

2. EXPERIMENTAL SECTION

2.1. Materials, Instrumentation, and Physical Measure- 144
ments. Sodium diclofenac, indomethacin, salicylaldoxime, $MnCl_2 \cdot$ 145
 $4H_2O$, $Mn(ClO_4)_2 \cdot 6H_2O$, MeONa, and KOH were purchased from 146
Sigma-Aldrich, and all solvents were purchased from Chemlab. All 147
chemicals and solvents were reagent grade and were used as purchased 148
without any further purification. **Caution!** Perchlorate salts can be 149
explosive and should be handled with care. 150

Infrared spectra ($400–4000\text{ cm}^{-1}$) were recorded on a Nicolet 151
FT-IR 6700 spectrometer with samples prepared as relatively smaller 152
KBr disks. UV-vis spectra were recorded as Nujol mulls and in 153
DMSO solution at concentrations in the range of $10^{-5}–10^{-3}\text{ M}$ on 154
a Hitachi U-2001 dual-beam spectrophotometer. Room-temperature 155
magnetic measurements for complexes 3 and 4 were carried out on a 156
magnetic susceptibility balance from Sherwood Scientific (Cambridge, 157
U.K.). C, H, and N elemental analyses were performed on a PerkinElmer 158
240B elemental analyzer. Molar conductivity measurements of 1 mM 159
DMSO solution of the complexes were carried out with a Crison Basic 160
30 conductometer. 161

Magnetic measurements for complexes 1 and 2 were carried out in 162
the Unitat de Mesures Magnètiques (Universitat de Barcelona) with a 163
Quantum Design SQUID MPMS-XL magnetometer equipped with 164
a 5 T magnet. Pascal's constants were used to estimate diamagnetic 165
corrections to the molar paramagnetic susceptibility. The magnetic 166
data analysis and fittings were carried out using the PHI program. 167

2.2. Synthesis of the Complexes. **2.2.1. Synthesis of** $[\text{Mn}_6(\text{O})_2(\text{dicl})_2(\text{sao})_6(\text{MeOH})_6]$ (**1**). A methanolic solution (10 mL) containing H_2sao (41 mg, 0.3 mmol) and MeONa (32 mg, 0.6 mmol) was stirred for 1 h and added simultaneously with a methanolic solution (10 mL) of Nadcl (29 mg, 0.4 mmol) to a methanolic solution (10 mL) of $\text{Mn}(\text{ClO}_4)_2 \cdot 6\text{H}_2\text{O}$ (108 mg, 0.3 mmol). The resultant solution was left for slow evaporation after 1 h of stirring. Dark-brown well-formed crystals of $[\text{Mn}_6(\text{O})_2(\text{dicl})_2(\text{sao})_6(\text{MeOH})_6]$ (59 mg, 60%) suitable for X-ray structure determination were collected after a week. Anal. Calcd for $[\text{Mn}_6(\text{O})_2(\text{dicl})_2(\text{sao})_6(\text{MeOH})_6]$ (**1**) ($\text{C}_{76}\text{H}_{74}\text{Cl}_4\text{Mn}_6\text{N}_8\text{O}_{24}$) (MW = 1954.84): C 46.69, H 3.82, N 5.73; found C 46.51, H 4.01, N 5.95. IR (KBr pellet), $\nu_{\text{max}}/\text{cm}^{-1}$: $\nu(\text{C}=\text{N})_{\text{sao}}$ 1598 (very strong (vs)); $\nu(\text{N}-\text{O})_{\text{sao}}$ 1440 (strong (s)); $\nu_{\text{asym}}(\text{CO}_2)_{\text{dicl}}$ 1586 (vs); $\nu_{\text{sym}}(\text{CO}_2)_{\text{dicl}}$ 1388 (vs); $\Delta\nu(\text{CO}_2) = \nu_{\text{asym}}(\text{CO}_2) - \nu_{\text{sym}}(\text{CO}_2) = 198 \text{ cm}^{-1}$. UV-vis, as a Nujol mull, λ/nm : 648(shoulder (sh)), 385 (sh), 287. In DMSO, λ/nm ($\epsilon/\text{M}^{-1}\text{cm}^{-1}$): 650 (580), 390 (1900), 289 (14 000). The compound is soluble in *N,N*-dimethylformamide (DMF) and dimethyl sulfoxide (DMSO) ($\Lambda_{\text{M}} = 8 \text{ S}\cdot\text{cm}^2\cdot\text{mol}^{-1}$, in 1 mM DMSO solution).

2.2.2. Synthesis of $[\text{Mn}_6(\text{O})_2(\text{indo})_2(\text{sao})_6(\text{H}_2\text{O})_4]$ (2**).** Complex **2** was prepared by a similar procedure. More specifically, a methanolic solution (30 mL) of indomethacin (36 mg, 0.1 mmol), MeONa (38 mg, 0.7 mmol), and H_2sao (41 mg, 0.3 mmol) was stirred for 1 h and added to a methanolic solution (10 mL) of $\text{Mn}(\text{ClO}_4)_2 \cdot 6\text{H}_2\text{O}$ (108 mg, 0.3 mmol). The resultant solution was stirred for 1 h and left for slow evaporation. Dark-brown crystals of $[\text{Mn}_6(\text{O})_2(\text{indo})_2(\text{sao})_6(\text{H}_2\text{O})_4]$ (**2**) (72 mg, 70%) suitable for X-ray structure determination were collected after a week. Anal. Calcd for $[\text{Mn}_6(\text{O})_2(\text{indo})_2(\text{sao})_6(\text{H}_2\text{O})_4]$ (**2**) ($\text{C}_{80}\text{H}_{72}\text{Cl}_2\text{Mn}_6\text{N}_8\text{O}_{28}$) (MW = 1993.96): C 48.19, H 3.64, N 5.73; found C 47.89, H 3.82, N 5.73. IR (KBr pellet), $\nu_{\text{max}}/\text{cm}^{-1}$: $\nu(\text{C}=\text{N})_{\text{sao}}$ 1598 (vs); $\nu(\text{N}-\text{O})_{\text{sao}}$ 1439 (s); $\nu_{\text{asym}}(\text{CO}_2)_{\text{indo}}$ 1560 (vs); $\nu_{\text{sym}}(\text{CO}_2)_{\text{indo}}$ 1373 (vs); $\Delta\nu(\text{CO}_2) = 187 \text{ cm}^{-1}$. UV-vis, as a Nujol mull, λ/nm : 650 (sh), 312 (sh), 287. In DMSO, λ/nm ($\epsilon/\text{M}^{-1}\text{cm}^{-1}$): 647 (600), 316 (sh) (4500), 290 (13 500). The compound is soluble in methanol, DMF, and DMSO ($\Lambda_{\text{M}} = 6 \text{ S}\cdot\text{cm}^2\cdot\text{mol}^{-1}$ in 1 mM DMSO solution) and partially soluble in H_2O .

2.2.3. Synthesis of $[\text{Mn}(\text{dicl})_2(\text{MeOH})_4]$ (3**).** Complex **3** was prepared by the addition of Nadcl (159 mg, 0.5 mmol) dissolved in MeOH (10 mL) to a methanolic solution (10 mL) of $\text{MnCl}_2 \cdot 4\text{H}_2\text{O}$ (0.25 mmol, 50 mg) followed by 1 h of stirring. The colorless microcrystalline product of $[\text{Mn}(\text{dicl})_2(\text{MeOH})_4]$ (100 mg, 55%) was collected after 2 weeks from the resultant solution. Anal. Calcd for $[\text{Mn}(\text{dicl})_2(\text{MeOH})_4]$ ($\text{C}_{32}\text{H}_{36}\text{Cl}_4\text{MnN}_2\text{O}_8$) (MW = 773.40): C 49.70, H 4.69, N 3.62; found C 49.57, H 4.52, N 3.73. IR (KBr pellet), $\nu_{\text{max}}/\text{cm}^{-1}$: $\nu_{\text{asym}}(\text{CO}_2)_{\text{dicl}}$ 1587 (vs); $\nu_{\text{sym}}(\text{CO}_2)_{\text{indo}}$ 1379 (vs); $\Delta\nu(\text{CO}_2) = 208 \text{ cm}^{-1}$. UV-vis, as a Nujol mull, λ/nm : 290. In DMSO, λ/nm ($\epsilon/\text{M}^{-1}\text{cm}^{-1}$): 290 (22 000). μ_{eff} at room temperature = $2.15 \text{ } 5.95\mu_{\text{B}}$. The complex is soluble in methanol, DMF, and DMSO ($\Lambda_{\text{M}} = 9 \text{ S}\cdot\text{cm}^2\cdot\text{mol}^{-1}$ in 1 mM DMSO solution).

2.2.4. Synthesis of $[\text{Mn}(\text{indo})_2(\text{MeOH})_4]$ (4**).** A methanolic solution (10 mL) containing indomethacin (180 mg, 0.5 mmol) and KOH (0.5 mmol, 28 mg) was stirred for 1 h in order to deprotonate indomethacin. The solution was added dropwise to a methanolic solution (10 mL) of $\text{MnCl}_2 \cdot 4\text{H}_2\text{O}$ (0.25 mmol, 50 mg) and the resultant solution was stirred for 30 min. Colorless microcrystalline product of $[\text{Mn}(\text{indo})_2(\text{MeOH})_4]$ (125 mg, 60%) precipitated after 10 days and was collected by filtration. Anal. Calcd for $[\text{Mn}(\text{indo})_2(\text{MeOH})_4]$ ($\text{C}_{42}\text{H}_{46}\text{Cl}_2\text{MnN}_2\text{O}_{12}$) (MW = 896.68): C 56.26, H 5.17, N 3.12; found C 55.96, H 5.01, N 3.21. IR (KBr pellet), $\nu_{\text{max}}/\text{cm}^{-1}$: $\nu_{\text{asym}}(\text{CO}_2)_{\text{indo}}$ 1599 (vs); $\nu_{\text{sym}}(\text{CO}_2)_{\text{indo}}$ 1392 (vs); $\Delta\nu(\text{CO}_2) = 207 \text{ cm}^{-1}$; UV-vis, as a Nujol mull, λ/nm : 318 (sh), 275. In DMSO, λ/nm ($\epsilon/\text{M}^{-1}\text{cm}^{-1}$): 320 (10 500), 277 (20 900). μ_{eff} at room temperature = $6.05\mu_{\text{B}}$. The complex is soluble in methanol, DMF, and DMSO ($\Lambda_{\text{M}} = 8 \text{ S}\cdot\text{cm}^2\cdot\text{mol}^{-1}$ in 1 mM DMSO solution).

2.3. X-ray Structure Determination. Single crystals from compounds **1** and **2** were selected, separated from their mother liquor, and mounted on a Bruker Kappa APEX 2 diffractometer equipped with a triumph monochromator using $\text{Mo K}\alpha$ radiation. Cell dimension refinement was accomplished using the settings of at least 120 high θ reflections with $I \geq 20\sigma(I)$. The crystals presented no decay during

the data collection. The frames collected (running φ and ω scans) were integrated with the Bruker SAINT Software package⁷⁵ using a narrow-frame algorithm. Data were corrected using the SADABS program.⁷⁶ The structures were solved by the SUPERFLIP package⁷⁷ incorporated into Crystals. The Crystals version 14.40 program package⁷⁸ has been used for the refinement and all subsequent calculations through full-matrix least squares on F^2 . All non-hydrogen atoms, except the disordered water oxygen atoms, have been refined anisotropically. All hydrogen atoms were found at their expected positions and refined using proper riding constraints to the pivot atoms. Molecular illustrations were drawn using CAMERON.⁷⁹ Crystallographic details are summarized in Table S1.

3. RESULTS AND DISCUSSION

3.1. Synthesis Considerations. Structurally characterized compounds **1** and **2** consist of two inverse-[9-MC-3] cores accommodating diclofenac or indomethacin anions, respectively, and show similar geometrical features. Complexes **1** and **2** were isolated in high yield by the reaction of a mixture containing equimolar quantities of $\text{Mn}(\text{ClO}_4)_2 \cdot 6\text{H}_2\text{O}$ and sao^{2-} in methanol in the presence of sodium salt of the NSAID in a $\text{Mn}^{2+}/\text{sao}^{2-}/\text{NSAID}^-$ ratio of 3:3:1 at room temperature. The isolated compounds are crystalline and dark brown and are soluble in DMSO, being nonelectrolytes ($\Lambda_{\text{M}} = 6\text{--}8 \text{ S}\cdot\text{cm}^2\cdot\text{mol}^{-1}$, 1 mM in DMSO).

Compounds **3** and **4** were prepared via the aerobic reaction of $\text{MnCl}_2 \cdot 4\text{H}_2\text{O}$ with the sodium salt of the NSAID in methanol in a 1:2 $\text{Mn}^{2+}/\text{NSAID}^-$ ratio at room temperature. The colorless compounds are soluble in DMSO and nonelectrolytes ($\Lambda_{\text{M}} = 8\text{--}9 \text{ S}\cdot\text{cm}^2\cdot\text{mol}^{-1}$, 1 mM in DMSO).

Complexes **1**–**4** were characterized by elemental analysis, IR and UV-vis spectroscopy, and magnetic measurements. The structures of compounds **1** and **2** were determined by X-ray crystallography.

3.2. Structures of Complexes 1 and 2. Structurally characterized compounds **1** and **2** consist of two inverse-[9-MC-3] metallacrown cores accommodating diclofenac or indomethacin anions, respectively, and show similar geometrical features. Each [9-MC-3] metallacrown ring consists of three Mn(III) atoms and three salicylaldoximate ligands as the constructing ligands. The salicylaldoximate ligands are doubly deprotonated (sao^{2-}) and act as tridentate binucleating ligands being coordinated to a Mn(III) atom via the salicylato oxygen (O_{sal}) and oximate nitrogen forming a six-membered chelate ring and to an adjacent Mn(III) atom via the oximate oxygen (O_{ox}) (Figure 2). The unit $[\text{Mn}-\text{N}-\text{O}_{\text{ox}}]$ is repeated three times, creating the nine-membered metallacrown ring. The metallacrown core is characterized as inverse because the manganese(III) atoms, instead of the oxygen atoms, are oriented toward the central cavity.

3.2.1. Crystal Structure of Complex 1. The molecular structure of complex **1** is depicted in Figure 3, and important bond lengths and angles are given in Tables 1 and S2, respectively. The complex consists of two [9-MC-3] metallacrown rings, two diclofenac ligands, and six methanol ligands. The specific connectivity of the atoms forming the ring is $\text{Mn}(1)-\text{O}(2)-\text{N}(3)-\text{Mn}(4)-\text{O}(12)-\text{N}(11)-\text{Mn}(6)-\text{O}(19)-\text{N}(20)$, and the average bond distances of the ring are $\text{Mn}-\text{O}_{\text{ox}} = 1.918 \text{ \AA}$ (in the range 1.896(2)–1.9404(17) Å), $\text{Mn}-\text{N} = 1.996 \text{ \AA}$ (in the range 1.991(2)–2.003(2) Å), and $\text{N}-\text{O}_{\text{ring}} = 1.372 \text{ \AA}$ (in the range 1.360(3)–1.386(3) Å). The bond valence sum values for the Mn atoms in complex **1** are 3.05 (for Mn1), 3.03 (for Mn4), and 2.96 (for Mn6) and verify

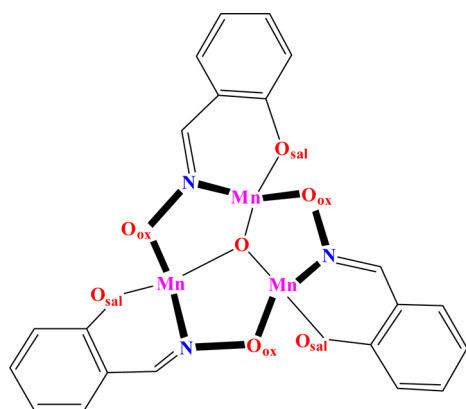


Figure 2. [9-MC-3] metallacrown ring found in the structures of complexes **1** and **2**.

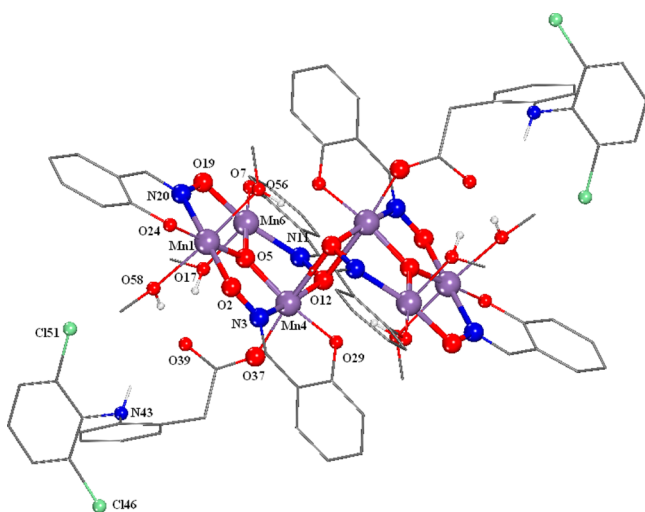


Figure 3. Molecular structure of complex **1**.

Table 1. Selected Bond Distances in Complex **1**

bonds	bond distance (Å)	bond atoms	bond distance (Å)
Mn(1)–O(2)	1.905(2)	Mn(4)–O(5)	1.8796(17)
Mn(1)–O(5)	1.8938(17)	Mn(4)–O(12)	1.9404(17)
Mn(1)–O(24)	1.864(2)	Mn(4)–O(12)′	2.4629(19)
Mn(1)–O(56)	2.302(3)	Mn(4)–O(37)	2.1082(19)
Mn(1)–O(58)	2.277(2)	Mn(4)–O(29)	1.8973(18)
Mn(1)–N(20)	1.993(2)	Mn(4)–N(3)	1.991(2)
Mn(6)–O(5)	1.8792(17)	Mn(6)–O(17)	2.166(2)
Mn(6)–O(7)	1.8560(19)	Mn(6)–O(19)	1.896(2)
Mn(6)–N(11)	2.003(2)	O(12)–N(11)	1.386(3)
O(2)–N(3)	1.360(3)	O(19)–N(20)	1.369(3)
Mn(1)⋯Mn(4)	3.2604(6)	Mn(1)⋯Mn(6)	3.2591(7)
Mn(4)⋯Mn(6)	3.2590(6)	Mn(4)⋯Mn(4)′	3.3827(5)

299 that all Mn atoms are in the +3 oxidation state, as calculated by
300 the Pauling equation:^{80,81}

$$\sum S_{ij} = \sum \exp \frac{R_0 - R_{ij}}{b} \quad (1)$$

302 where R_{ij} is the length, S_{ij} is the valence of the bond between
303 atoms i and j , and R_0 and b are the empirically determined bond
304 valence parameters (for Mn, $R_0 = 1.75$ and $b = 0.37$).⁸² The
305 ring Mn(III)⋯Mn(III) separation distance is 3.26 Å with the

three ring Mn(III) atoms forming an equilateral triangle. The
crystal structure of the complex contains two nine-membered
inverse metallacrown rings of the type [9-MC_{Mn(III)N(sal)}-3] in a
stepladder-like arrangement. The metallacrown rings are
bonded via two ring oximate oxygen atoms (O(12) and
O(12)′), creating the binuclear moiety [Mn(4)–O(12)–
Mn(4)′–O(12)′] with a planar arrangement [the sum of
the angles O(12)–Mn(4)–O(12)′ (= 80.31(7)°), Mn(4)′–
O(12)–Mn(4) (= 99.69(7)°), O(12)–Mn(4)′–O(12)′
(= 80.31(7)°), and Mn(4)′–O(12)′–Mn(4) (= 99.69(7)°) is
almost 360.0(7)°] and a Mn(4)⋯Mn(4)′ distance equal to
3.3827(5) Å. The arrangement of the six Mn(III) atoms of the
complex is distorted trigonal antiprismatic with the three
Mn(III) atoms of each metallacrown ring forming the bases;
the bases' centroid-to-centroid distance is equal to 4.876 Å, and
the bases' plane-to-plane distance is 3.006 Å. Taking into
consideration the average ionic radius of Mn(III) (= 0.75 Å),⁸³
the space in the metallacrown cavity is such that it allows
the encapsulation of an O²⁻ ligand (ionic radius = 1.26 Å),⁸³
which is bound to the three ring Mn(III) atoms at an average
Mn–O(5) distance of 1.8865 Å (in the range 1.8792(17)–
1.8938(17) Å), and it is almost coplanar with the three Mn(III)
atoms of the metallacrown ring (~0.10 Å out of the Mn(III)₃
plane).

The coordination environment and the geometry of the
Mn(III) atoms are different. Mn(1) and Mn(4) bear a NO₅
chromophore and have a Jahn–Teller distorted octahedral
geometry with the Jahn–Teller axis being vertical to the plane
formed from the three Mn(III) atoms, i.e., Mn(1), Mn(4), and
Mn(6) atoms. Mn(1) has a planar structure with four short
distances (Mn(1)–(N/O)_{av} = 1.914 Å) and two long distances
(Mn(1)–O_{av} = 2.289 Å), exhibiting an elongated octahedral
geometry with atoms O(2), O(5), O(24), and N(20) located at
the equatorial positions of the octahedron and O(56) and
O(58) lying at the axial positions of the octahedron. Mn(4)
also has a planar configuration with four short distances
(Mn(4)–(N/O)_{av} = 1.927 Å) with O(5), O(12), O(29), and
N(3), which form the basis of the octahedron, an intermediate
(Mn(4)–O(37) = 2.1082(19) Å), and a long distance
(Mn(4)–O(12)′ = 2.4635(18) Å) where atoms O(37) and
O(12)′ are located at the axial positions of the asymmetrically
elongated octahedron. Mn(6) has a NO₄ coordination
environment with a slight distortion from the regular square-
based pyramidal geometry as concluded from the value of the
trigonality index,⁸⁴ $\tau = (177.39(8) - 169.69(9))/60 = 0.128$
[$\tau = (\varphi_1 - \varphi_2)/60^\circ$, where φ_1 and φ_2 are the largest angles in
the coordination sphere; $\tau = 0$ for a perfect square pyramid;
 $\tau = 1$ for a perfect trigonal bipyramid]. N(11), O(5), O(7), and
O(19) form the basis of the square pyramid, and O(17) lies at
the apex of the pyramid. The elongation of the tetragonal
pyramid on Mn(6) also has the same orientation with respect
to the Jahn–Teller axis on Mn(1) and Mn(4).

The two diclofenac ligands are deprotonated by being
monodentately bound to Mn(4) via the carboxylato oxygen
atoms O(37) [Mn(4)–O(37) = 2.1082(19) Å]. The coordina-
tion spheres of Mn(6) and Mn(1) are completed by one and
two O_M atoms, respectively, from the six methanol ligands of
the complex at an average Mn–O_M distance of 2.234 Å (in the
range 2.166(2)–2.302(2) Å).

3.2.2. Crystal Structure of Complex **2**. The molecular
structure of complex **2** is depicted in Figure 4, and important
bond lengths and angles are given in Tables 2 and S3, respec-
tively. The complex consists of two [9-MC-3] metallacrown

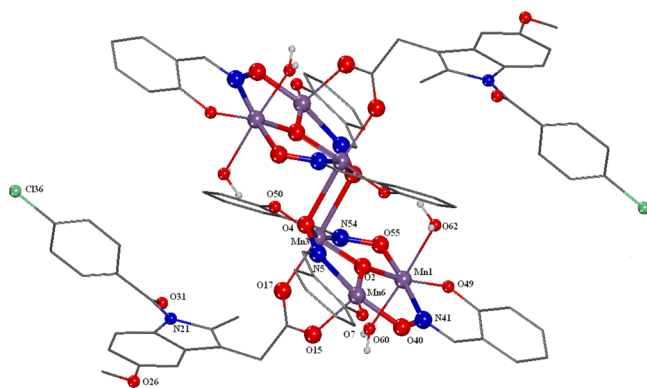


Figure 4. Molecular structure of complex 2.

Table 2. Selected Bond Distances in Complex 2

bonds	bond distance (Å)	bond atoms	bond distance (Å)
Mn(1)–O(2)	1.8994(15)	Mn(3)–O(2)	1.8716(14)
Mn(1)–O(49)	1.8788(17)	Mn(3)–O(4)′	2.4458(17)
Mn(1)–O(55)	1.9242(16)	Mn(3)–O(4)	1.9581(17)
Mn(1)–O(60)	2.219(2)	Mn(3)–O(17)	2.1462(17)
Mn(1)–O(62)	2.412(2)	Mn(3)–O(50)	1.8906(15)
Mn(1)–N(41)	2.0075(19)	Mn(3)–N(54)	2.029(2)
Mn(6)–O(2)	1.8828(16)	Mn(6)–O(40)	1.8953(15)
Mn(6)–O(7)	1.8652(17)	Mn(6)–N(5)	2.0297(18)
Mn(6)–O(15)	2.1137(19)	O(55)–N(54)	1.377(2)
O(4)–N(5)	1.379(2)	O(40)–N(41)	1.364(2)
Mn(1)⋯Mn(6)	3.2863(12)	Mn(1)⋯Mn(3)	3.2927(11)
Mn(3)⋯Mn(6)	3.1610(13)	Mn(3)⋯Mn(3)′	3.4247(15)

369 rings, two indomethacin ligands, and four aqua ligands. The
 370 arrangement and the coordination of the saO^{2-} ligands in the
 371 inverse metallacrown ring of complex 2 are similar to that of
 372 complex 1. The connectivity of the atoms forming the ring is
 373 Mn(1)–O(55)–N(54)–Mn(3)–O(4)–N(5)–Mn(6)–
 374 O(40)–N(41), and the average bond distances of the ring are
 375 Mn–O_{ox} = 1.923 Å, Mn–N = 2.022 Å, and N–O_{ring} = 1.373 Å.
 376 The bond valence sum values for the Mn atoms in complex 2 as
 377 calculated with eq 1 are 2.95 (for Mn1), 2.94 (for Mn3), and
 378 2.95 (for Mn6), verifying that the oxidation state of all Mn
 379 atoms is +3. In contrast to 1, the three ring Mn(III)⋯Mn(III)
 380 separation distances are not equal, having an average distance of
 381 3.247 Å with two almost equal distances (Mn(1)⋯Mn(3) =
 382 3.2927(11) Å and Mn(1)⋯Mn(6) = 3.2863(12) Å) forming an iso-
 383 scles triangle (the third side is Mn(3)⋯Mn(6) = 3.1610(13) Å).
 384 The two ring oximate oxygen atoms (O(4) and O(4)′) are
 385 the bridging atoms between the two nine-membered metal-
 386 lacrown rings forming the binuclear moiety [Mn(3)–O(4)–
 387 Mn(3)′–O(4)′] with a distance Mn(3)⋯Mn(3)′ = 3.4247(15)
 388 Å, and the sum of the four angles is 360.00(8)° (O(4)–
 389 Mn(3)–O(4)′ = 78.49(8)°, Mn(3)–O(4)–Mn(3)′ =
 390 101.51(8)°, O(4)–Mn(3)′–O(4)′ = 78.49(8)°, and Mn(3)–
 391 O(4)′–Mn(3)′ = 101.51(8)°), which indicates a planar
 392 arrangement. The distorted trigonal antiprismatic arrangement
 393 of the six Mn(III) atoms of the complex has a centroid-to-
 394 centroid distance between the two bases formed by the three
 395 Mn(III) atoms of each metallacrown ring equal to 5.302 Å and
 396 a plane-to-plane distance equal to 3.240 Å. Oxygen atom O(2)
 397 is the encapsulated O²⁻ ligand in the metallacrown cavity
 398 1.8846 Å (average distance) from the three ring Mn(III) atoms,
 399 and it is displaced ~0.18 Å out of the [Mn(III)₃] plane.

Mn(1) and Mn(3) have a NO₅ coordination environment
 with a distorted octahedral geometry. Mn(1) has a planar
 configuration with four short distances (Mn(1)–(N/O)_{av} =
 1.927 Å) and two long distances (Mn(1)–O_{av} = 2.302 Å),
 exhibiting a Jahn–Teller elongated octahedral geometry with
 O(2), O(55), O(49), and N(51) located at the equatorial
 positions of the octahedron and O(60) and O(62) lying at the
 axial positions of the octahedron. The configuration of Mn(3)
 with four short distances (Mn(3)–(N/O)_{av} = 1.8979 Å) and
 two long distances (Mn(3)–O(17) = 2.1462(17) Å, Mn(3)–
 O(4)′ = 2.4458(17) Å) with O(2), O(4), O(50) and N(54) is
 similar, forming the basal plane of the octahedron, with O(4)′
 and O(17) being at the apical positions of the asymmetri-
 cally elongated octahedron. Mn(6) with a NO₄ chromophore
 presents a slightly distorted square-based pyramidal geometry
 with a value of the trigonality index of $\tau = (166.89(8) -$
 $164.43(8))/60 = 0.041$, where N(5), O(2), O(7), and O(40)
 form the basis of the square pyramid and O(15) lies at the apex
 of the pyramid.

The two deprotonated indomethacin ligands are bidentate
 $\mu_{1,3}$ -bridging ligands bound to Mn(3) and Mn(6) via the car-
 boxylato oxygen atoms O(17) (Mn(3)–O(17) = 2.1462(17) Å)
 and O(15) (Mn(6)–O(15) = 2.1137(19) Å), respectively. The
 coordination sphere of Mn(1) is completed by two O_w atoms
 from the aqua ligands at an average Mn(1)–O_w distance of
 2.316 Å.

**3.3. Spectroscopic Characterization of the Com-
 plexes.** The IR spectra of complexes 1 and 2 exhibit char-
 acteristic bands attributed to $\nu(\text{C}=\text{N})_{\text{pyridyl}}$ (1598 cm⁻¹) and
 $\nu(\text{N}=\text{O})$ (1439–1440 cm⁻¹) of the saO^{2-} ligand participating
 in the formation of the metallacrown ring.⁴⁷ Additionally, in the
 IR spectra of complexes 1–4, the bands attributed to the
 antisymmetric and the symmetric stretching vibrations,
 $\nu_{\text{asym}}(\text{CO}_2)$ and $\nu_{\text{sym}}(\text{CO}_2)$ of the carboxylato groups of the
 NSAID ligands, are located at 1560–1599 and 1373–
 1392 cm⁻¹, respectively. The difference $\Delta\nu(\text{CO}_2)$ [$=\nu_{\text{asym}}(\text{CO}_2)$
 $-\nu_{\text{sym}}(\text{CO}_2)$] is a useful characteristic tool for determining the
 coordination mode of the carboxylato ligands.⁸⁵ For complexes
 1, 3, and 4, $\Delta\nu(\text{CO}_2)$ is found in the range 198–208 cm⁻¹ and
 higher than that found in the sodium salt of the corresponding
 NSAID ($\Delta\nu(\text{CO}_2) = 192\text{--}194$ cm⁻¹), indicating an asym-
 metric monodentate binding mode of the carboxylato group of
 the NSAID,⁸⁶ whereas for complex 2, the calculated $\Delta\nu(\text{CO}_2)$
 value is 187 cm⁻¹, suggesting the existence of a bidentate
 coordination mode.^{85,86}

The UV–vis spectra of the complexes were recorded as
 Nujol mull and in DMSO solution and are similar, suggest-
 ing that the complexes retain their structure in solution.
 In addition, the complexes do not dissociate in solution ($\Lambda_{\text{M}} =$
 $6\text{--}9$ S·cm²·mol⁻¹) and have the same UV–vis spectral patterns
 in DMSO solution and in the presence of the buffer solution
 used in the biological experiments, suggesting that they keep
 their integrity in solution.^{47,87}

3.4. Magnetic Measurements of the Compounds.

3.4.1. dc Magnetic Measurements of Compound 1. The
 temperature dependence of the susceptibility data in the form
 of $\chi_{\text{M}}T$ for complex 1 is shown in Figure 5. The value of $\chi_{\text{M}}T$ at
 room temperature is 16.428 cm³·mol⁻¹·K and increases while
 the temperature decreases to the value of 20.982 cm³·mol⁻¹·K
 at 10 K. After that temperature, there is an abrupt decrease to
 the value of 7.776 cm³·mol⁻¹·K at 2 K. The overall magnetic
 behavior of this complex is ferromagnetic, whereas at low
 temperatures the zero-field effect is important.

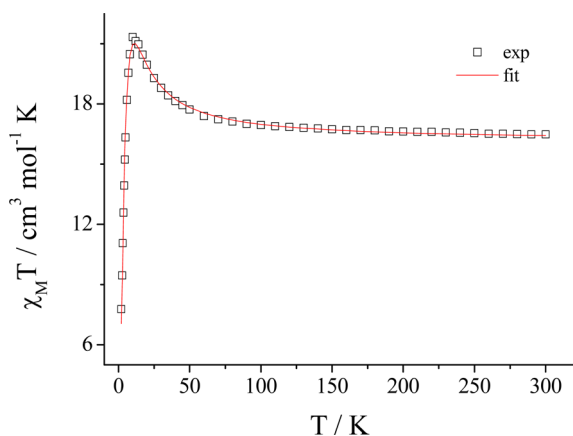


Figure 5. Temperature dependence of the susceptibility data in the form of $\chi_M T$ vs T for complex **1**. The solid line represents the fitting results according to the magnetic model shown in eq 2 (details in the text).

463 According to the literature,^{88–91} torsion angles above 31° will
 464 promote ferromagnetic coupling, whereas below 31° anti-
 465 ferromagnetic coupling is revealed. Two of the three torsion
 466 angles between the Mn(III) ions are smaller than 31° (Mn(1)–
 467 N(20)–O(19)–Mn(6) = 16.72° , Mn(1)–O(2)–N(3)–
 468 Mn(4) = 19.23° , Mn(4)–O(12)–N(11)–Mn(6) = 32.28°),
 469 indicating that the magnetic interactions through the oximato
 470 bridge are antiferromagnetic and the interactions between
 471 the Mn(4)–Mn(6)/Mn(4')–Mn(6') and between the Mn(4)–
 472 Mn(4') ions are ferromagnetic. Thus, the Hamiltonian chosen to
 473 fit the magnetic susceptibility data is shown in eq 2 and
 474 contains J_1 between the Mn(4)–Mn(6)/Mn(4')–Mn(6') and
 475 J_3 between the Mn(4)–Mn(4') ions as a ferromagnetic
 476 exchange constant whereas J_2 (oximato bridge) as is the AFM
 477 one (the magnetic model is shown in Figure S1). The values of
 478 J_1 , J_2 , J_3 , and g obtained from the fitting process (solid line in
 479 Figure 5) are $J_1 = +0.89 \text{ cm}^{-1}$, $J_2 = -0.17 \text{ cm}^{-1}$, $J_3 = +1.28 \text{ cm}^{-1}$,
 480 and $g = 1.92$, in agreement with those reported in the
 481 literature.^{88–91}

$$H = -2J_1(S_4S_6 + S_4'S_6') - 2J_2(S_1S_4 + S_4S_6 + S_1'S_4' + S_4'S_6') - 2J_3S_4S_4' \quad (2)$$

483 According to the fitting results of the susceptibility data, the
 484 ground state of the system is $S = 4$ with many low excited states
 485 ($S = 5$ at 0.8 cm^{-1} , $S = 6$ at 1.9 cm^{-1}), indicating a nonisolated
 486 ground state. This was further confirmed by the lack of fitting
 487 results of the magnetization data at 2 K using the giant spin
 488 model (Figure S2).

489 **3.4.2. Alternating Current Magnetic Measurements of**
 490 **Compound 1.** Dynamic ac magnetization measurements with
 491 frequencies ν in the 10–1500 Hz range have been performed in
 492 order to clarify the nature of the magnetic state of compound **1**
 493 and are shown in Figure 6. The thermal variation of the
 494 ac susceptibility shows rounded peaks for both the real and
 495 imaginary parts, whereas for both components a second peak
 496 seems to appear. Both in-phase and out-of-phase components
 497 show strong frequency-dependent behavior. χ' and χ'' shift to
 498 lower temperatures for lower frequencies, which is expected for
 499 an SMM. The temperature dependence of the relaxation time
 500 $\tau(t)$ follows the Arrhenius law: $\tau(t) = \tau_0 \exp(U_{\text{eff}}/k_B T)$ and is
 501 shown in Figure 6 in the form of $\ln(\tau)$ versus $1/T$, where τ_0 is a
 502 prefactor and U_{eff} is the activation barrier. The fitted procedure

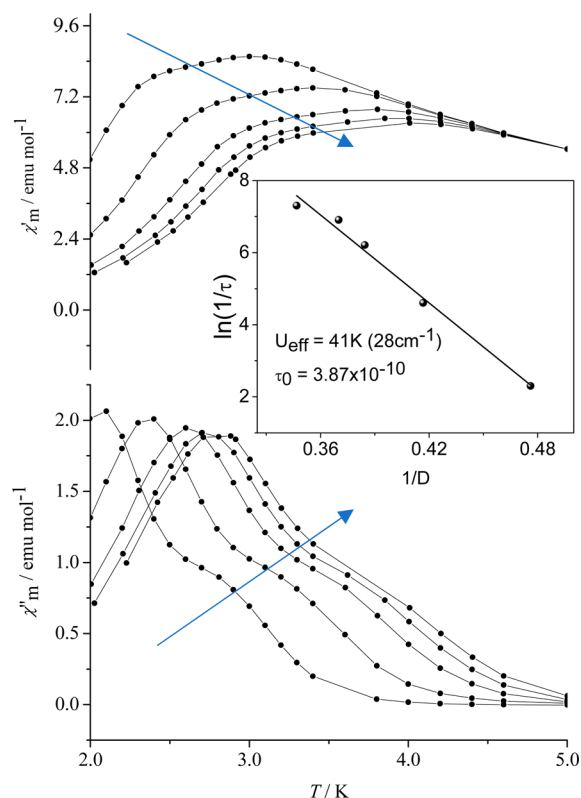


Figure 6. Temperature dependence ac magnetic susceptibility (real χ' and imaginary χ'' susceptibility components) for compound **1** in an oscillating field of 5 Oe and a 0 dc field and for frequencies 10, 100, 500, 1000, 1500 Hz. (The arrow shows the trend in frequencies starting from the lowest value, i.e., 10 Hz). The inset shows the Arrhenius plot with the fitting results. (See the text for details.)

gave the values $U_{\text{eff}}/k_B = 41 \text{ K}$ and $\tau_0 = 3.87 \times 10^{-10} \text{ s}$ in the
 range expected for SMM systems.^{88–91}

3.4.3. dc Magnetic Measurements of Compound 2. The
 temperature dependence of the susceptibility data in the form
 of $\chi_M T$ for complex **2** is shown in Figure 7. The value of $\chi_M T$ at
 room temperature is $16.853 \text{ cm}^3 \cdot \text{mol}^{-1} \cdot \text{K}$ and decreases with the
 decrease in temperature to a minimum of $7.358 \text{ cm}^3 \cdot \text{mol}^{-1} \cdot \text{K}$ at
 14 K. After that temperature, there is an abrupt increase to the
 value of $11.046 \text{ cm}^3 \cdot \text{mol}^{-1} \cdot \text{K}$ at 2 K. The overall magnetic

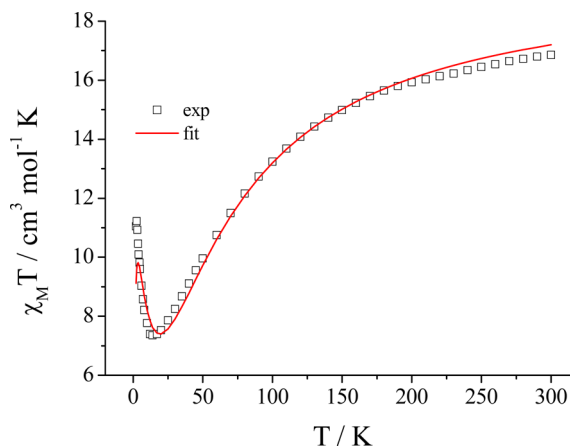


Figure 7. Temperature dependence of the susceptibility data in the form of $\chi_M T$ vs T for complex **2**. The solid line represents the fitting results according to eq 3. (See text for details.)

512 behavior of this complex is antiferromagnetic. Two torsion
 513 angles between the Mn(III) ions are smaller than 31° (Mn(1)–
 514 N(41)–O(40)–Mn(6) = 7.60° , Mn(6)–N(5)–O(4)–Mn(3) =
 515 15.93°), which may promote antiferromagnetic interactions
 516 between these magnetic ions. AFM interactions are also favored
 517 because of the *syn-syn*-carboxylato bridges in the complex. The
 518 existence of a torsion angle higher than 31° (Mn(1)–O(55)–
 519 N(54)–Mn(3) = 32.23°) may give rise to ferromagnetic inter-
 520 actions between the Mn(1)–Mn(3) ions. Since there is a
 521 *syn-syn*-carboxylate bridge, which would give AFM coupling,
 522 and a torsion angle of 32.23° between Mn(1) and Mn(3)
 523 ions that promotes FM coupling, a $4J$ exchange coupling
 524 Hamiltonian was tried ($H = -2J_1(S_3S_6 + S_3'S_6') - 2J_2(S_1S_6 +$
 525 $S_1'S_6') - 2J_3S_3S_3' - 2J_4(S_1S_3 + S_1'S_3')$). However, the fitting
 526 results led to the same AFM values for J_1 and J_4 . Thus, the fit
 527 was finally performed with a $3J$ Hamiltonian described by eq 3,
 528 and the magnetic model is shown in Figure S3. As can be
 529 observed, the only FM coupling (J_3) takes place between
 530 Mn(3) and Mn(3'), whereas the expected FM between Mn(1)
 531 and Mn(3) (due to the torsion angle) is not observed. The
 532 oximate and *syn-syn*-carboxylate bridges give rise to the AFM
 533 coupling J_2 and J_1 , respectively.

$$H = -2J_1(S_3S_6 + S_3'S_6') - 2J_2(S_1S_6 + S_1'S_6' + S_1'S_3') - 2J_3S_3S_3' \quad (3)$$

534
 535 The values of the J_1 , J_2 , J_3 , and g obtained from the fitting pro-
 536 cess (solid line in Figure 7) are $J_1 = -1.27 \text{ cm}^{-1}$, $J_2 = -4.9 \text{ cm}^{-1}$,
 537 $J_3 = +1.4 \text{ cm}^{-1}$, and $g = 2.09$, in agreement with those reported
 538 in the literature.^{88–91}

539 According to the fitting results of the susceptibility data, the
 540 ground state of the system is $S = 4$, which is not well iso-
 541 lated from the next excited $S = 3$ state (4.3 cm^{-1}). Fitting
 542 of the magnetization data at 2 K using a giant spin model of an
 543 $S = 4$ spin gave poor results (Figure S4).

544 No ac signals were observed for this compound, indicating a
 545 non-SMM character.

546 **3.4.4. Room Temperature Magnetic Measurements for**
 547 **Compounds 3 and 4.** The magnetic measurements for com-
 548 plexes 3 and 4 were performed at room temperature. The
 549 observed values $\mu_{\text{eff}} (= 5.95\text{--}6.05 \mu_{\text{B}})$ for the complexes are
 550 close to the spin-only value ($= 5.92 \text{ MB}$) at room temperature
 551 and are typical for mononuclear high-spin Mn(II) complexes
 552 with a d^5 configuration ($S = 5/2$).^{92,93}

553 **3.5. Proposed Structures for Complexes 3 and 4.**
 554 Despite our efforts (diverse solvents and mixtures of them as
 555 well as diverse crystallization conditions were used), we did not
 556 manage to get single crystals of complexes 3 and 4 suitable for
 557 X-ray crystallography. Therefore, we have characterized these
 558 complexes on the basis of existing elemental analysis, magnetic
 559 measurements, and IR spectroscopic data. According to the
 560 results derived from the room-temperature magnetic data,
 561 complexes 3 and 4 are neutral mononuclear. According to
 562 IR spectroscopic data, the NSAID ligands are deprotonated and
 563 are bound to the manganese ion in a monodentate fashion via a
 564 carboxylato oxygen atom. Complexes 3 and 4 are expected to
 565 have similar structures with complex $[\text{Mn}(\text{nif})_2(\text{MeOH})_4]$,⁷²
 566 where Hnif is NSAID niflumic acid being coordinated to Mn in
 567 a monodentate mode. Similarly, complexes 3 and 4 have a
 568 MnO_6 chromophore and the centrosymmetric coordination
 569 sphere around the six-coordinate Mn consists of two oxygens
 570 from the NSAID ligands and four oxygen atoms from the
 571 methanol ligands (Figure 8).

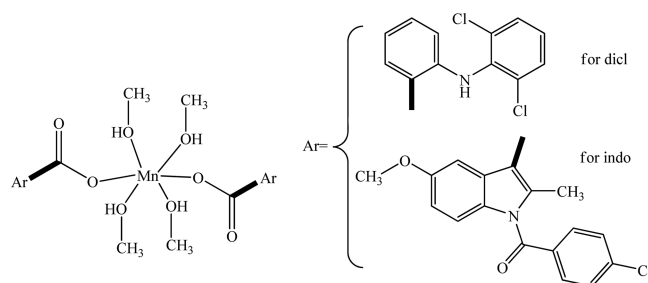


Figure 8. Proposed structures for complexes 3 and 4.

4. CONCLUSIONS

In our search for multifunctional materials that may exhibit,
 besides single-molecule magnetism, important biological
 activity, we investigated the interaction of $\text{Mn}(\text{ClO}_4)_2$ with
 doubly deprotonated salicylaldoxime in the presence of the
 NSAIDs sodium diclofenac or indomethacin resulting in the
 formation of the hexanuclear Mn(III) clusters $[\text{Mn}_6(\text{O})_2(\text{dicl})_2(\text{sao})_6(\text{CH}_3\text{OH})_6]$ (1) or $[\text{Mn}_6(\text{O})_2(\text{indo})_2(\text{sao})_6(\text{H}_2\text{O})_4]$ (2) respectively, which both may also be characterized as
 stepladder inverse-9-metallacrown-3 complexes. Furthermore,
 compound 1 is characterized as a single-molecule magnet,
 exhibiting strong frequency-dependent behavior with an
 activation barrier of $U_{\text{eff}} = 41 \text{ K}$, whereas compound 2 has
 overall antiferromagnetic behavior and non-SMM character. The
 mononuclear Mn(II) complexes $[\text{Mn}(\text{dicl})_2(\text{CH}_3\text{OH})_4]$ (3) and
 $[\text{Mn}(\text{indo})_2(\text{CH}_3\text{OH})_4]$ (4) were isolated upon interaction of
 Mn(II) with the NSAIDs. The present compounds 1 and 2 are
 the first manganese metallacrowns hosting nonsteroidal anti-
 inflammatory drugs. Studies concerning the biological relevance
 of such metallacrowns are quite rare in the literature;^{47,94–97}
 therefore, such studies of the synthesized complexes may possi-
 bly lead to the design of more potent therapeutic compounds.

ASSOCIATED CONTENT

Supporting Information

The Supporting Information is available free of charge on the ACS Publications website at DOI: 10.1021/acs.inorgchem.7b00655.

Tables containing the crystallographic data and selected bond distances and angles for complexes 1 and 2, magnetic models for complexes 1 and 2 used to describe the Hamiltonian model, and plots with the reduced magnetization data for complexes 1 and 2 (PDF)

Accession Codes

CCDC 1536792 and 1536793 contain the supplementary crystallographic data for this paper. These data can be obtained free of charge via www.ccdc.cam.ac.uk/data_request/cif, or by emailing data_request@ccdc.cam.ac.uk, or by contacting The Cambridge Crystallographic Data Centre, 12 Union Road, Cambridge CB2 1EZ, UK; fax: +44 1223 336033.

AUTHOR INFORMATION

Corresponding Authors

*E-mail: vtango@upatras.gr. (V. Tangoulis)
 *E-mail: gepsomas@chem.auth.gr. (G. Psomas)

ORCID

Vassilis Tangoulis: 0000-0002-2039-2182

George Psomas: 0000-0002-5879-7265

Notes

The authors declare no competing financial interest.

618 ■ REFERENCES

- (1) For details see <http://metamodern.com/2009/12/29/theres-plenty-of-room-at-the-bottom%E2%80%9D-feynman-1959/>.
- (2) Chittipeddi, S.; Cromack, K. R.; Miller, J. S.; Epstein, A. J. Ferromagnetism in molecular decamethylferrocenium tetracyanoethenide (DMeFc TCNE). *Phys. Rev. Lett.* **1987**, *58*, 2695–2698.
- (3) Christou, G.; Gatteschi, D.; Hendrickson, D. N.; Sessoli, R. Single-molecule magnets. *MRS Bull.* **2000**, *25*, 66–71.
- (4) Bircher, R.; Chaboussant, G.; Dobe, C.; Gudel, H. U.; Ochsenein, S. T.; Sieber, A.; Waldmann, O. Single-Molecule Magnets Under Pressure. *Adv. Funct. Mater.* **2006**, *16*, 209–220.
- (5) Murrie, M.; Price, D. J. Molecular magnetism. *Annu. Rep. Prog. Chem., Sect. A: Inorg. Chem.* **2007**, *103*, 20–38.
- (6) Leuenberger, M. N.; Loss, D. Quantum computing in molecular magnets. *Nature* **2001**, *410*, 789–793.
- (7) Ardavan, A.; Rival, O.; Morton, J. J. L.; Blundell, S. J.; Tyryshkin, A. M.; Timco, G. A.; Winpenny, R. E. P. Will Spin-Relaxation Times in Molecular Magnets Permit Quantum Information Processing? *Phys. Rev. Lett.* **2007**, *98*, 057201.
- (8) Gomez-Romero, P.; Sanchez, C. *Functional Hybrids Materials*; Wiley-VCH Verlag GmbH & Co. KGaA: Weinheim, Germany, 2004; pp 15–44.
- (9) Weigert, E. C.; South, J.; Rykov, S. A.; Chen, J. G. Multifunctional composites containing molybdenum carbides as potential electrocatalysts. *Catal. Today* **2005**, *99*, 285–290.
- (10) Galán-Mascarós, J. R.; Coronado, E. Molecule-based ferromagnetic conductors: Strategy and design. *C. R. Chim.* **2008**, *11*, 1110–1116.
- (11) Torquato, S.; Hyun, S.; Donev, A. Multifunctional Composites: Optimizing Microstructures for Simultaneous Transport of Heat and Electricity. *Phys. Rev. Lett.* **2002**, *89*, 266601.
- (12) MasPOCH, D.; Ruiz-Molina, D.; Veciana, J. Old materials with new tricks: multifunctional open-framework materials. *Chem. Soc. Rev.* **2007**, *36*, 770–818.
- (13) Gaspar, A. B.; Ksenofontov, V.; Seredyuk, M.; Guetlich, P. Multifunctionality in spin crossover materials. *Coord. Chem. Rev.* **2005**, *249*, 2661–2676.
- (14) Coronado, R.; Galán-Mascarós, J. R.; Romero, F. *Functional Hybrids Materials*; Wiley-VCH Verlag GmbH & Co. KGaA: Weinheim, Germany, 2004; pp 317–346 and references therein.
- (15) Pecoraro, V. L.; Stemmler, A. J.; Gibney, B. R.; Bodwin, J. J.; Wang, H.; Kampf, J. W.; Barwinski, A. Metallacrowns: A New Class of Molecular Recognition Agents. *Prog. Inorg. Chem.* **1996**, *45*, 83–177.
- (16) Mezei, G.; Zaleski, C. M.; Pecoraro, V. L. Structural and Functional Evolution of Metallacrowns. *Chem. Rev.* **2007**, *107*, 4933–5003.
- (17) Verani, C. N.; Bothe, E.; Burdinski, D.; Weyhermüller, T.; Florke, U.; Chaudhuri, P. Synthesis, Structure, Electrochemistry, and Magnetism of $[\text{Mn}^{\text{III}}\text{Mn}^{\text{III}}]$, $[\text{Mn}^{\text{III}}\text{Fe}^{\text{III}}]$ and $[\text{Fe}^{\text{III}}\text{Fe}^{\text{III}}]$ Cores: Generation of Phenoxyl Radical Containing $[\text{Fe}^{\text{III}}\text{Fe}^{\text{III}}]$ Species. *Eur. J. Inorg. Chem.* **2001**, *2001*, 2161–2169.
- (18) Chaudhuri, P.; Rentschler, E.; Birkelbach, F.; Krebs, C.; Bill, E.; Weyhermüller, T.; Flörke, U. Ground Spin State Variation in Carboxylate-Bridged Tetranuclear $[\text{Fe}_2\text{Mn}_2\text{O}_2]^{8+}$ Cores and a Comparison with Their $[\text{Fe}_4\text{O}_2]^{8+}$ and $[\text{Mn}_4\text{O}_2]^{8+}$ Congeners. *Eur. J. Inorg. Chem.* **2003**, *2003*, 541–555.
- (19) Inglis, R.; Milios, C. J.; Jones, L. F.; Piligkos, S.; Brechin, E. K. Twisted molecular magnets. *Chem. Commun.* **2012**, *48*, 181–190.
- (20) Yang, C.; Cheng, K.; Hung, S.; Nakano, M.; Tsai, H. Crystal packing effects within $[\text{Mn}^{\text{III}}_3\text{O}]^{7+}$ single-molecule magnets: Controlling intermolecular antiferromagnetic interactions. *Polyhedron* **2011**, *30*, 3272–3278.
- (21) Holynska, M.; Pietzonka, C.; Dehnen, S. Synthesis and Properties of Complexes with Unusual $\{\text{Mn}^{\text{III}}_4\}$ and $\{\text{Mn}^{\text{II}}_4\}$ Cages. *Z. Anorg. Allg. Chem.* **2011**, *637*, 556–561.
- (22) Inglis, R.; Jones, L. F.; Mason, K.; Collins, A.; Moggach, S. A.; Parsons, S.; Perlepes, S. P.; Wernsdorfer, W.; Brechin, E. K. Ground Spin State Changes and 3D Networks of Exchange Coupled $[\text{Mn}^{\text{III}}_3]$ Single-Molecule Magnets. *Chem. - Eur. J.* **2008**, *14*, 9117–9121.
- (23) Raptopoulou, C. P.; Boudalis, A. K.; Lazarou, K. N.; Psycharis, V.; Panopoulos, N.; Fardis, M.; Diamantopoulos, G.; Tchuagues, J.-P.; Mari, A.; Papavassiliou, G. Salicylaldehyde in manganese(III) carboxylate chemistry: Synthesis, structural characterization and physical studies of hexanuclear and polymeric complexes. *Polyhedron* **2008**, *27*, 3575–3586.
- (24) Song, X.; Liu, R.; Zhang, S.; Li, L. A rare ferromagnetic manganese(III) hexanuclear cluster. *Inorg. Chem. Commun.* **2010**, *13*, 828–830.
- (25) Milios, C. J.; Inglis, R.; Vinslava, A.; Bagai, R.; Wernsdorfer, W.; Parsons, S.; Perlepes, S. P.; Christou, G.; Brechin, E. K. Toward a Magnetostructural Correlation for a Family of Mn_6 SMMs. *J. Am. Chem. Soc.* **2007**, *129*, 12505–12511.
- (26) Yang, C.; Cheng, K.; Nakano, M.; Lee, G.; Tsai, H. Synthesis, structures and magnetic properties of two hexanuclear complexes. *Polyhedron* **2009**, *28*, 1842–1851.
- (27) Geng, J.; Wang, Z.; Li, M.; Xiao, H. A hexanuclear manganese(III) complex constructed from triangular-shaped $[\text{Mn}_3\text{O}]$ units with azide bridge. *Polyhedron* **2011**, *30*, 3134–3136.
- (28) Yang, C.; Hung, S.; Lee, G.; Nakano, M.; Tsai, H. Slow Magnetic Relaxation in an Octanuclear Manganese Chain. *Inorg. Chem.* **2010**, *49*, 7617–7619.
- (29) Yang, C.; Feng, P.; Chen, Y.; Tsai, Y.; Lee, G.; Tsai, H. Molecular architecture based on manganese triangles: Monomer, dimer, and one-dimensional polymer. *Polyhedron* **2011**, *30*, 3265–3271.
- (30) Duffy, C. P.; Elliott, C. J.; O'Connor, R. A.; Heenan, M. M.; Coyle, S.; Cleary, I. M.; Kavanagh, K.; Verhaegen, S.; O'Loughlin, C. M.; NicAmhlaoibh, R.; Clynes, M. Enhancement of chemotherapeutic drug toxicity to human tumor cells *in vitro* by a subset of non-steroidal anti-inflammatory drugs (NSAIDs). *Eur. J. Cancer* **1998**, *34*, 1250–1259.
- (31) Weder, J. E.; Dillon, C. T.; Hambley, T. W.; Kennedy, B. J.; Lay, P. A.; Biffin, J. R.; Regtop, H. L.; Davies, N. M. Copper complexes of non-steroidal anti-inflammatory drugs: an opportunity yet to be realized. *Coord. Chem. Rev.* **2002**, *232*, 95–126.
- (32) Amin, A. R.; Vyas, P.; Attur, M.; Leszczynskapiziak, J.; Patel, I. R.; Weissmann, G.; Abramson, S. B. The mode of action of aspirin-like drugs: effect on inducible nitric oxide synthase. *Proc. Natl. Acad. Sci. U. S. A.* **1995**, *92*, 7926–7930.
- (33) Kim, K.; Yoon, J.; Kim, J. K.; Baek, S. J.; Eling, T. E.; Lee, W. J.; Ryu, J.; Lee, J. G.; Lee, J.; Yoo, J. Cyclooxygenase Inhibitors Induce Apoptosis in Oral Cavity Cancer Cells by Increased Expression of Nonsteroidal Anti-Inflammatory Drug-Activated Gene. *Biochem. Biophys. Res. Commun.* **2004**, *325*, 1298–1303.
- (34) Woo, D. H.; Han, I.; Jung, G. Mefenamic acid-induced apoptosis in human liver cancer cell-lines through caspase-3 pathway. *Life Sci.* **2004**, *75*, 2439–2449.
- (35) Smith, M.; Hawcroft, G.; Hull, M. A. The effect of non-steroidal anti-inflammatory drugs on human colorectal cancer cells: evidence of different mechanisms of action. *Eur. J. Cancer* **2000**, *36*, 664–674.
- (36) Inoue, A.; Muranaka, S.; Fujita, H.; Kanno, T.; Tamai, H.; Utsumi, K. Molecular mechanism of diclofenac-induced apoptosis of promyelocytic leukemia: dependency on reactive oxygen species, akt, bid, cytochrome and caspase pathway. *Free Radical Biol. Med.* **2004**, *37*, 1290–1299.
- (37) Zhang, T.; Otevreil, T.; Gao, Z.; Gao, Z.; Ehrlich, S. M.; Fields, J. Z.; Boman, B. M. Evidence That APC Regulates Survivin Expression: A Possible Mechanism Contributing to the Stem Cell Origin of Colon Cancer. *Cancer Res.* **2001**, *61*, 8664–8667.
- (38) Banti, C. N.; Hadjikakou, S. K. on-Steroidal Anti-Inflammatory Drugs (NSAIDs) in Metal Complexes and Their Effect at the Cellular Level. *Eur. J. Inorg. Chem.* **2016**, *2016*, 3048–3071.
- (39) Psoomas, G.; Kessissoglou, D. P. Quinolones and non-steroidal antiinflammatory drugs interacting with copper(II), nickel(II), cobalt(II) and zinc(II): Structural features, biological evaluation and perspectives. *Dalton Trans.* **2013**, *42*, 6252–6276.
- (40) Etcheverry, S. B.; Barrio, D. A.; Cortizo, A. M.; Williams, P. A. M. Three new vanadyl(IV) complexes with non-steroidal anti-

- 756 inflammatory drugs (Ibuprofen, Naproxen and Tolmetin). Bioactivity
757 on osteoblast-like cells in culture. *J. Inorg. Biochem.* **2002**, *88*, 94–100.
- 758 (41) Weder, J. E.; Hambley, T. W.; Kennedy, B. J.; Lay, P. A.; Foran,
759 G. J.; Rich, A. M. Determination of the Structures of Antiinflammatory
760 Copper(II) Dimers of Indomethacin by Multiple-Scattering Analyses
761 of X-ray Absorption Fine Structure Data. *Inorg. Chem.* **2001**, *40*,
762 1295–1302.
- 763 (42) Reynolds, J. E. F.; Martindale, W. *The Extra Pharmacopoeia*, 31st
764 ed.; The Pharmaceutical Press: London, 1996.
- 765 (43) Boothe, D. M. In *Veterinary Pharmacology and Therapeutics*;
766 Adams, H.R., Ed.; 8th ed; Iowa State University Press: Ames, IA, 2001;
767 pp 433–435.
- 768 (44) Dimiza, F.; Perdih, F.; Tangoulis, V.; Turel, I.; Kessissoglou, D.
769 P.; Psomas, G. Interaction of copper(II) with the non-steroidal anti-
770 inflammatory drugs naproxen and diclofenac: Synthesis, Structure,
771 DNA- and albumin-binding. *J. Inorg. Biochem.* **2011**, *105*, 476–489.
- 772 (45) Kovala-Demertzi, D.; Theodorou, A.; Demertzis, M. A.;
773 Raptopoulou, C. P.; Terzis, A. Synthesis and characterization of
774 tetrakis- μ -2-[(2,6-dichlorophenyl)amino]benzeneacetodiaquo-
775 dicopper(II) dihydrate and tetrakis- μ -2-[(2,6-dichlorophenyl)amino]-
776 benzeneaceto dimethyl-formamidodicopper(II). *J. Inorg. Biochem.*
777 **1997**, *65*, 151–157.
- 778 (46) Castellari, C.; Feroci, G.; Ottani, S. Diclofenac interactions:
779 tetrakis[μ -2-(2,6-dichloro-anilino)phenylacetato]-1:2 κ^8 O:O'-diacetone-
780 1 κ O,2 κ O-dicopper(II)(Cu-Cu) acetaldehyde solvate. *Acta Crystallogr.*
781 *Sect. C: Cryst. Struct. Commun.* **1999**, *55*, 907–910.
- 782 (47) Tarushi, A.; Raptopoulou, C. P.; Psycharis, V.; Kontos, C. K.;
783 Kessissoglou, D. P.; Scorilas, A.; Tangoulis, V.; Psomas, G. Copper(II)
784 inverse-[9-metallacrown-3] compounds accommodating nitrate or
785 diclofenac ligands: structure, magnetism and biological activity. *Eur. J.*
786 *Inorg. Chem.* **2016**, *2016*, 219–231.
- 787 (48) Zampakou, M.; Tangoulis, V.; Raptopoulou, C. P.; Psycharis, V.;
788 Papadopoulos, A. N.; Psomas, G. Structurally diverse manganese(II)-
789 diclofenac complexes showing enhanced antioxidant activity and
790 affinity to serum albumins in comparison to sodium diclofenac. *Eur. J.*
791 *Inorg. Chem.* **2015**, *2015*, 2285–2294.
- 792 (49) Zampakou, M.; Hatzidimitriou, A. G.; Papadopoulos, A. N.;
793 Psomas, G. Neutral and cationic manganese(II)-diclofenac complexes:
794 Structure and biological evaluation. *J. Coord. Chem.* **2015**, *68*, 4355–
795 4372.
- 796 (50) Kovala-Demertzi, D.; Mentzafos, D.; Terzis, A. Metal complexes
797 of the anti-inflammatory drug sodium [2-[(2,6-dichlorophenyl)-
798 amino]phenyl]acetate (diclofenac sodium). Molecular and crystal
799 structure of cadmium diclofenac. *Polyhedron* **1993**, *12*, 1361–1370.
- 800 (51) Kourkoumelis, N.; Demertzis, M. A.; Kovala-Demertzi, D.;
801 Koutsodimou, A.; Moukarika, A. Preparations and spectroscopic
802 studies of organotin complexes of diclofenac. *Spectrochim. Acta, Part A*
803 **2004**, *60*, 2253–2259.
- 804 (52) Kyropoulou, M.; Raptopoulou, C. P.; Psycharis, V.; Psomas, G.
805 Ni(II) complexes with non-steroidal anti-inflammatory drug diclofe-
806 nac: Structure and interaction with DNA and albumins. *Polyhedron*
807 **2013**, *61*, 126–136.
- 808 (53) Mosca, F.; Bray, M.; Lattanzio, M.; Fumagalli, M.; Tosetto, C.
809 Comparative evaluation of the effects of indomethacin and ibuprofen
810 on cerebral perfusion and oxygenation in preterm infants with patent
811 ductus arteriosus. *J. Pediatr.* **1997**, *131*, 549–554.
- 812 (54) Weser, U.; Sellinger, K.; Lengfelder, E.; Werner, W.; Strahle, J.
813 Structure of Cu₂(indomethacin)₄ and the reaction with superoxide in
814 aprotic systems. *Biochim. Biophys. Acta, Gen. Subj.* **1980**, *631*, 232–245.
- 815 (55) Weder, J. E.; Hambley, T. W.; Kennedy, B. J.; Lay, P. A.;
816 MacLachlan, D.; Bramley, R.; Delfs, C. D.; Murray, K. S.; Moubaraki,
817 B.; Warwick, B.; Biffin, J. R.; Regtop, H. L. Anti-Inflammatory
818 Dinuclear Copper(II) Complexes with Indomethacin. Synthesis,
819 Magnetism and EPR Spectroscopy. Crystal Structure of the N,N-
820 Dimethylformamide Adduct. *Inorg. Chem.* **1999**, *38*, 1736–1744.
- 821 (56) Morgan, Y. R.; Turner, P.; Kennedy, B. J.; Hambley, T. W.; Lay,
822 P. A.; Biffin, J. R.; Regtop, H. L.; Warwick, B. Preparation and
823 characterization of dinuclear copper-indomethacin anti-inflammatory
824 drugs. *Inorg. Chim. Acta* **2001**, *324*, 150–161.
- (57) Tarushi, A.; Raptopoulou, C. P.; Psycharis, V.; Kessissoglou, D. 825
P.; Papadopoulos, A. N.; Psomas, G. Structure and biological 826
perspectives of Cu(II)-indomethacin complexes. *J. Inorg. Biochem.* 827
2014, *140*, 185–198. 828
- (58) Galani, A.; Kovala-Demertzi, D.; Kourkoumelis, N.; 829
Koutsodimou, A.; Dokorou, V.; Ciunik, Z.; Russo, U.; Demertzis, M. 830
A. Organotin adducts of indomethacin: synthesis, crystal structures 831
and spectral characterization of the first organotin complexes of 832
indomethacin. *Polyhedron* **2004**, *23*, 2021–2030. 833
- (59) Larson, E. J.; Pecoraro, V. L. In *Manganese Enzymes*; Pecoraro, V. 834
L., Ed.; VCH Publishers Inc: New York, 1992; pp 1–28. 835
- (60) Mullins, C. S.; Pecoraro, V. L. Reflections on small molecule 836
manganese models that seek to mimic photosynthetic water oxidation 837
chemistry. *Coord. Chem. Rev.* **2008**, *252*, 416–443. 838
- (61) Guo, Z.; Sadler, P. J. Metals in Medicine. *Angew. Chem., Int. Ed.* 839
1999, *38*, 1512–1531. 840
- (62) Li, M.; Chen, C.; Zhang, D.; Niu, J.; Ji, B. Mn(II), Co(II) and 841
Zn(II) complexes with heterocyclic substituted thiosemicarbazones: 842
Synthesis, characterization, X-ray crystal structures and antitumor 843
comparison. *Eur. J. Med. Chem.* **2010**, *45*, 3169–3177. 844
- (63) Zhou, D.; Chen, Q.; Qi, Y.; Fu, H.; Li, Z.; Zhao, K.; Gao, J. 845
Anticancer Activity, Attenuation on the Absorption of Calcium in 846
Mitochondria, and Catalase Activity for Manganese Complexes of N- 847
Substituted Di(picolyl)amine. *Inorg. Chem.* **2011**, *50*, 6929–6937. 848
- (64) Qiu-Yun, C.; Dong-Fang, Z.; Juan, H.; Wen-Jie, G.; Jing, G. 849
Synthesis, anticancer activities, interaction with DNA and mitochon- 850
dria of manganese complexes. *J. Inorg. Biochem.* **2010**, *104*, 1141– 851
1147. 852
- (65) Dorkov, P.; Pantcheva, I.; Sheldrick, W.; Mayer-Figge, H.; 853
Petrova, R.; Mitewa, M. Synthesis, structure and antimicrobial activity 854
of manganese(II) and cobalt(II) complexes of the polyether ionophore 855
antibiotic Sodium Monensin A. *J. Inorg. Biochem.* **2008**, *102*, 26–32. 856
- (66) Mandal, S.; Rout, A.; Ghosh, A.; Pilet, G.; Bandyopadhyay, D. 857
Synthesis, structure and antibacterial activity of manganese(III) 858
complexes of a Schiff base derived from furfurylamine. *Polyhedron* 859
2009, *28*, 3858–3862. 860
- (67) Zampakou, M.; Akrivou, M.; Andreadou, E. G.; Raptopoulou, C. 861
P.; Psycharis, V.; Pantazaki, A. A.; Psomas, G. Manganese(II) 862
complexes with quinolone antimicrobial agents oxolinic acid and 863
enrofloxacin: Structure, antimicrobial activity, DNA- and albumin- 864
binding. *J. Inorg. Biochem.* **2013**, *121*, 88–99. 865
- (68) Zampakou, M.; Balala, S.; Perdih, F.; Kalogiannis, S.; Turel, I.; 866
Psomas, G. Structure, antimicrobial activity, albumin- and DNA- 867
binding of manganese(II)-sparfloxacinato complexes. *RSC Adv.* **2015**, 868
5, 11861–11872. 869
- (69) Singh, D. P.; Kumar, K.; Sharma, C. New 14-membered 870
octaazamacrocyclic complexes: Synthesis, spectral, antibacterial and 871
antifungal studies. *Eur. J. Med. Chem.* **2010**, *45*, 1230–1236. 872
- (70) Zampakou, M.; Rizeq, N.; Tangoulis, V.; Papadopoulos, A. N.; 873
Perdih, F.; Turel, I.; Psomas, G. Manganese(II) complexes with the 874
non-steroidal anti-inflammatory drug tolfenamic acid: Structure and 875
biological perspectives. *Inorg. Chem.* **2014**, *53*, 2040–2052. 876
- (71) Feng, J.; Du, X.; Liu, H.; Sui, X.; Zhang, C.; Tang, Y.; Zhang, J. 877
Manganese-mefenamic acid complexes exhibit high lipoxygenase 878
inhibitory activity. *Dalton Trans.* **2014**, *43*, 10930–10939. 879
- (72) Tsiliki, P.; Perdih, F.; Turel, I.; Psomas, G. Structure, DNA- and 880
albumin-binding of the manganese(II) complex with the non-steroidal 881
antiinflammatory drug niflumic acid. *Polyhedron* **2013**, *53*, 215–222. 882
- (73) Tarushi, A.; Kakoulidou, C.; Raptopoulou, C. P.; Psycharis, V.; 883
Kessissoglou, D. P.; Zoi, I.; Papadopoulos, A. N.; Psomas, G. Zinc 884
complexes of diflunisal: Synthesis, characterization, structure, anti- 885
oxidant activity, and *in vitro* and *in silico* study of the interaction with 886
DNA and albumins. *J. Inorg. Biochem.* **2017**, *170*, 85–97. 887
- (74) Chilton, N. F.; Anderson, R. P.; Turner, L. D.; Soncini, A.; 888
Murray, K. S. PHI: A powerful new program for the analysis of 889
anisotropic monomeric and exchange-coupled polynuclear *d*- and *f*- 890
block complexes. *J. Comput. Chem.* **2013**, *34*, 1164–1175. 891
- (75) Bruker Analytical X-ray Systems, Inc. Apex2, Version 2 User 892
Manual, M86-E01078, Madison, WI, 2006. 893

- 894 (76) Siemens Industrial Automation, Inc. SADABS: Area-Detector
895 Absorption Correction; Madison, WI, 1996.
- 896 (77) Betteridge, P. W.; Carruthers, J. R.; Cooper, R. I.; Prout, K.;
897 Watkin, D. J. CRYSTALS version 12: software for guided crystal
898 structure analysis. *J. Appl. Crystallogr.* **2003**, *36*, 1487.
- 899 (78) Palatinus, L.; Chapuis, G. SUPERFLIP—a computer program for
900 the solution of crystal structures by charge flipping in arbitrary
901 dimensions. *J. Appl. Crystallogr.* **2007**, *40*, 786–790.
- 902 (79) Watkin, D. J.; Prout, C. K.; Pearce, L. J. CAMERON Program,
903 Chemical Crystallographic Laboratory, Oxford University: UK, 1996.
- 904 (80) Pauling, L. Atomic Radii and Interatomic Distances in Metals. *J.*
905 *Am. Chem. Soc.* **1947**, *69*, 542–553.
- 906 (81) Brown, I. D. Bond Valence Theory. *Struct. Bonding (Berlin, Ger.)*
907 **2013**, *158*, 11–58.
- 908 (82) Brown, I. D. Bond valence parameters, Information about
909 'bvparmxxxx.cif', 2016, [http://www.iucr.org/resources/data/datasets/](http://www.iucr.org/resources/data/datasets/bond-valence-parameters)
910 [bond-valence-parameters](http://www.iucr.org/resources/data/datasets/bond-valence-parameters).
- 911 (83) Shannon, R. D. Revised effective ionic radii and systematic
912 studies of interatomic distances in halides and chalcogenides. *Acta*
913 *Crystallogr., Sect. A: Cryst. Phys., Diffr., Theor. Gen. Crystallogr.* **1976**, *32*,
914 751–767.
- 915 (84) Addison, A. W.; Rao, T. N.; Reedijk, J.; van Rijn, J.; Verschoor,
916 G. C. Synthesis, structure, and spectroscopic properties of copper(II)
917 compounds containing nitrogen–sulphur donor ligands; the crystal
918 and molecular structure of aqua[1,7-bis(*N*-methylbenzimidazol-2'-yl)-
919 2,6-dithiaheptane] copper(II) perchlorate. *J. Chem. Soc., Dalton Trans.*
920 **1984**, 1349–1356.
- 921 (85) Nakamoto, K. *Infrared and Raman Spectra of Inorganic and*
922 *Coordination Compounds*, 6th ed.; Wiley: Hoboken, NJ, 2009; part B.
- 923 (86) Szorcisk, A.; Nagy, L.; Sletten, J.; Szalontai, G.; Kamu, E.; Fiore,
924 T.; Pellerito, L.; Kalman, E. Preparation and structural studies on
925 dibutyltin(IV) complexes with pyridine mono- and dicarboxylic acids.
926 *J. Organomet. Chem.* **2004**, *689*, 1145–1154.
- 927 (87) Dimiza, F.; Fountoulaki, S.; Papadopoulos, A. N.; Kontogiorgis,
928 C. A.; Tangoulis, V.; Raptopoulou, C. P.; Psycharis, V.; Terzis, A.;
929 Kessissoglou, D. P.; Psomas, G. Non-steroidal anti-inflammatory drug-
930 Copper(II) complexes: Structure and biological perspectives. *Dalton*
931 *Trans.* **2011**, *40*, 8555–8568.
- 932 (88) Milios, C. J.; Vinslava, A.; Wernsdorfer, W.; Prescimone, A.;
933 Wood, P. A.; Parsons, S.; Perlepes, S. P.; Christou, G.; Brechin, E. K.
934 Spin Switching via Targeted Structural Distortion. *J. Am. Chem. Soc.*
935 **2007**, *129*, 6547–6561.
- 936 (89) Inglis, R.; Jones, L. F.; Milios, C. J.; Datta, S.; Collins, A.;
937 Parsons, S.; Wernsdorfer, W.; Hill, S.; Perlepes, S. P.; Piligkos, S.;
938 Brechin, E. K. Attempting to understand (and control) the relationship
939 between structure and magnetism in an extended family of Mn₆ single-
940 molecule magnets. *Dalton Trans.* **2009**, 3403–3412.
- 941 (90) Jones, L. F.; Cochrane, M. E.; Koivisto, B. D.; Leigh, D. A.;
942 Perlepes, S. P.; Wernsdorfer, W.; Brechin, E. K. Tuning magnetic
943 properties using targeted structural distortion: New additions to a
944 family of Mn₆ single-molecule magnets. *Inorg. Chim. Acta* **2008**, *361*,
945 3420–3426.
- 946 (91) Tomsa, A.; Martínez-Lillo, J.; Li, Y.; Chamoreau, L.; Boubekeur,
947 K.; Farias, F.; Novak, M. A.; Cremades, E.; Ruiz, E.; Proust, A.;
948 Verdager, M.; Gouzerh, P. A new family of oxime-based hexanuclear
949 manganese(III) single molecule magnets with high anisotropy energy
950 barriers. *Chem. Commun.* **2010**, *46*, 5106–5108.
- 951 (92) Chiswell, B.; McKenzie, E. D.; Lindoy, L. F. In *Comprehensive*
952 *Coordination Chemistry*; Wilkinson, G., Ed.; Pergamon Press: Oxford,
953 1987; Vol. 4, p 1.
- 954 (93) Weatherburn, D. C.; Mandal, S.; Mukhopadhyay, S.; Bhaduri, S.;
955 Lindoy, L. F. In *Comprehensive Coordination Chemistry II*; McCleverty,
956 J. A.; Meyer, T. J. Eds.; Elsevier: Amsterdam, 2003; Vol. 5, p 1.
- 957 (94) Rajczak, E.; Gluszynska, A.; Juskowiak, B. Interaction of
958 metallacrown complexes with G-quadruplex DNA. *J. Inorg. Biochem.*
959 **2016**, *155*, 105–114.
- 960 (95) Afrati, T.; Pantazaki, A. A.; Dendrinou-Samara, C.;
961 Raptopoulou, C.; Terzis, A.; Kessissoglou, D. P. Copper inverse-9-
metallacrown-3 compounds interacting with DNA. *Dalton Trans.* **2010**, *39*, 765–775.
- (96) Dendrinou-Samara, C.; Papadopoulos, A. N.; Malamatari, D. A.;
Tarushi, A.; Raptopoulou, C. P.; Terzis, A. Samaras, E.; Kessissoglou,
D.P. Inter-conversion of 15-MC-5 to 12-MC-4 manganese metal-
lacrowns: structure and bioactivity of metallacrowns hosting
carboxylato complexes. *J. Inorg. Biochem.* **2005**, *99*, 864–875.
- (97) Alexiou, M.; Tsivikas, I.; Dendrinou-Samara, C.; Pantazaki, A.
A.; Trikalitis, P.; Lalioti, N.; Kyriakidis, D. A.; Kessissoglou, D. P. High
nuclearity nickel compounds with three, four or five metal atoms
showing antibacterial activity. *J. Inorg. Biochem.* **2003**, *93*, 256–264.